AAPS PharmSciTech (2020) 21: 318
DOI: 10.1208/s12249-020-01822-w

Research Article

Theme: Formulation and Delivery of Natural Products
Guest Editors: Harsh Chauhan, Abhijit Date and Sonali Dhindwal

Development and Evaluation of Astaxanthin as Nanostructure Lipid Carriers in Topical Delivery

Qiang Geng,[1] Yuming Zhao,[1] Lu Wang,[1] Lulu Xu,[1] Xiong Chen,[1] and Jing Han[1,2,3]

Received 22 April 2020; accepted 16 September 2020; published online 11 November 2020

Abstract. The study is designed to formulate, optimize, and evaluate astaxanthin (ASTA)-loaded nanostructured lipid carrier (NLC) with an aim to improve its stability, water solubility, skin permeability and retention and reduce drug-related side effects. ASTA was extracted from *Haematococcus pluvialis.* ASTA-NLC was formulated by the technique of melt emulsification—ultrasonic and optimized taking solid:liquid lipid ratio, total lipid:drug ratio, drug concentration, emulsifier types, and amounts as independent variables with particle sizes (PS) and entrapment efficiency (EE) as dependent variables. The optimized formulation (N21) exhibited spherical surfaced stable nanoparticles of 67.4 ± 2.1 nm size and 94.3 ± 0.5% EE. Formulation N21 was then evaluated for its physiological properties, physicochemical properties, drug content, *in vitro* release and skin penetration, and retention analysis. The ASTA-NLC was found to be nonirritating, homogenous, and with excellent stability and water solubility. *In vitro* release studies showed the cumulative release rate of NLC was 83.0 ± 3.4% at 48 h. The skin penetration and retention studies indicated that cumulative permeability was 174.10 ± 4.38 μg/cm^2 and the retention was 8.00 ± 1.62 μg/cm^2 within 24 h. It can be concluded that NLC serves as a promising carrier for site specific targeting with better stability and skin penetration.

KEY WORDS: astaxanthin; nanostructured lipid carriers; development; evaluation; transdermal absorption.

INTRODUCTION

The raising living standards boost the development of cosmeceuticals, especially with ingredients that reduce the oxidative stress and cellular damage of skin. Astaxanthin (ASTA, Fig. 1) is a lipid-soluble keto-carotenoid with superior antioxidant activity (1) and related anti-inflammatory/antiapoptotic effects both *in vitro* and *in vivo* (2). Other biological activities include anticancer (3), reduction of plasma cholesterol (4), relief of eyestrain (5), *etc.* Natural ASTA has been approved for the use as coloring agent for animal and aquatic feeds by different agencies such as the Food and Drug Administration (FDA) and European Commission. ASTA-rich natural resources, mainly *Haematococcus pluvialis*, have been used as food supplement regulated by European Commission (6) and National Medical Products Administration of China (7). The cosmetic benefits of ASTA result from different mechanisms: ASTA-induced decrease in nitric oxide synthase and apoptosis of keratinocytes (8) protects skin cells from ultraviolet-induced deterioration; reduction of up-regulation of matrix metalloproteinase-1 and skin fibroblast elastase slows skin aging (9); regulation of oxidative stress and inhibition of inflammatory cytokines relieve stimuli-induced inflammation (10), *etc.* Despite these therapeutic effects, the topical delivery of ASTA is hindered by its degradation susceptibility in the presence of light, heat, and oxygen. ASTA is also poorly water-soluble, and the crystallization of dissolve drug in physiological fluid may negatively influence the drug permeation across biological membranes. Therefore, in order to improve the bioavailability of ASTA for topical use, it is necessary to develop an inclusion formulation that can fulfill the multiple requirements of drug loading capacity, drug release profile, physiochemical stability, and drug permeation, so that it can be better applied in the cosmetic industry.

Guest Editors: Harsh Chauhan, Abhijit Date and Sonali Dhindwal

Supplementary Information The online version of this article (https://doi.org/10.1208/s12249-020-01822-w) contains supplementary material, which is available to authorized users.

[1] School of Pharmaceutical Engineering, Shenyang Pharmaceutical University, Benxi, 117004, China.
[2] School of Pharmaceutical Engineering, Shenyang Pharmaceutical University, NO.26, Huatuo Street, Xihu District, Benxi City, 117004, Liaoning Province, China.
[3] To whom correspondence should be addressed. (e–mail: Hj-8080@163.com)

Previous research have produced ASTA/natural DNA/chitosan nanoparticles (11), ASTA-loaded nanoemulsions (12), and ASTA liposomes (13) to improve the topical delivery of ASTA. The results have shown that the formulations, ranging from 80 to 400 nm, could improve the solubility, permeability, and chemical stability of ASTA to different degrees. Consequently, the therapeutic effects of ASTA, such as ultraviolet-induced skin photoaging phenomenon and melanin production, have been improved. These nano-sized dosage forms show promising transdermal delivery profiles for ASTA, establishing a fundamental foundation for the development of ASTA topical products. That being said, more types of nano-formulations are to be developed to further improve the aforementioned key parameters for the transdermal delivery of ASTA.

Solid lipid nanoparticle (SLN) is a type of biocompatible and biodegradable colloidal carrier (14,15) in which a drug payload is dissolved or dispersed in the solid lipid core of SLN covered with surface active agents. Compared with liposomes and polymeric micelles, preparations of SLN minimize the use of organic solvents, thereby with less concern in manufacture. It also has advantages (16,17) in protection of unstable drug and sustained or controlled release due to its rigid structure formed by hard lipid. However, a main drawback of SLN is the limited storage stability (18) as SLN is prone to crystal transformation (19) during the storage process, reducing the drug-lipid miscibility and therefore the drug loading efficiency. To overcome these deficiencies, nanostructured lipid carriers (NLC) (20) have been developed with effective improvements. The physical gap between the chains of triglyceride fatty acids and solid lipid within a matrix structure leaves more space for the carrier to accommodate drugs (21) and improve the stability (22) of the system. In terms of transdermal delivery, the small size (< 100 nm) and rheological property (23,24) of the NLC are also favorable characteristics. In addition, NLC has been validated with other cosmetic benefits including skin hydration, occlusion, enhanced bioavailability, and targeting effect upon specific surface modification (25). Several prior studies have shown the feasibility of preparing ASTA-NLC by characterizing its physiochemical properties and potential application as oral formulation. Therefore, it is hypothesized that ASTA can be effectively delivered through a transdermal route by formulating into ASTA-NLC with improved physiochemical properties.

The purpose of this study is to prepare ASTA into NLC formulations to effectively improve its physiochemical properties associated with the difficulty in transdermal delivery. ASTA-NLC formulations are optimized through the rational selections of lipid and emulsifying agents based on the NLC characteristics of particle size, encapsulation efficiency, and storage stability. The optimal formulation is assessed by its morphology, drug release profile, antioxidant activity, skin permeation, skin retention, and resistance to oxygen, heat, and ultraviolet. The study lays a fundamental foundation for the potential application of ASTA-NLC in the field of cosmeceuticals.

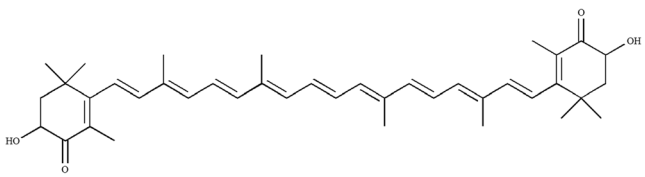

Fig. 1. Chemical structure of ASTA

MATERIALS AND METHODS

Materials and Animals

Reference standard of ASTA (> 98% purity) was acquired from Aladdin Corporation (Shanghai China). *Haematococcus pluvialis* powder was acquired from Jingzhou Natural ASTA Corporation (Hubei China). DL-Alpha-tocopherol (fat-soluble VE) was acquired from McLean Biochemical Technology Corporation (Shanghai, China). Glyceryl tribehenate (GTB) was acquired from Gaffarlion (France). Decanoyl/octanoyl-glycerides (Myl 812) and Pluronic F68 (F68) were acquired from MAYA Reagent (Jiaxing, Zhejiang). Cremophor EL 35 (EL 35) was acquired from BASF (Germany). The water used in this study was produced by a Laboratory Ultrapure Water System (Aquapro International Company, State of Delaware, USA). Other chemicals were of analytical grade.

Male Sprague Dawley rats (SD, 200 ± 10 g) and Kunming mice (KM, 20 ± 5 g) were acquired from the Center of Laboratory Animal Shenyang Pharmaceutical University (Liaoning, China). The protocol for animal experiment was approved by the Shenyang Pharmaceutical University Ethics Committee.

HPLC Method

In this study, the content of ASTA in all samples was determined using a HPLC method. ASTA standard reference (0.8 mg) was dissolved in methanol under ultrasonication to obtain a stock solution (10 mL). The stock solution was diluted by different times to obtain a series of ASTA solutions with known concentrations. Each solution was filtered by 0.45-μm nylon membrane, followed by the HPLC determination with the selected chromatographic parameters (Table I). The standard curve $Y = 39{,}923X + 2120.9$ ($n = 5$, $r^2 = 0.9998$) showed good linearity within 1 and 20 μg/mL, where X was the concentration of ASTA and Y was HPLC peak area. The HPLC method was applied to all samples in this study.

Preparation of ASTA

ASTA was prepared according to the previous method (26) with slight modifications. Briefly, *Haematococcus pluvialis* powder (5.00 g) was added to ethyl acetate-ethanol binary solvent (2:1, v/v, 80 mL) and placed in a beaker. Such sample was processed by an ultrasonic cell disruptor (Ningbo Scientz Biotechnology Co., Ltd) at 200 W for 5 min before it was filtered. The collected filtrate was dried under reduced pressure at 35°C in a rotary evaporator (Shanghai Yarong Biochemical Instrument Factory). The obtained ASTA ester was dissolved in ethanol (100 mL) and stored at 4°C until saponification. During saponification, ethanol solution (20 mL) of ASTA ester was added with a same volume of 80% ethanol solution containing 6 mg/L NaOH. The reaction

Table I. HPLC conditions for the determination of ASTA

Name	Condition
Chromatographic column	Supersil ODS 2 (4.6 mm × 250 mm, 5 μm)
Wavelength	476 nm
Mobile phase	Methanol:water (95:5, v/v)
Injection volume	10 μL
Flow rate	1.0 mL/min
Column temperature	25 °C

ASTA, astaxanthin; HPLC, high-performance liquid chromatography

system was filled with nitrogen and protected from light. After stirring at 1200 rpm for 50 min, saponified ASTA ester was added with ethyl acetate (5 mL) and distilled water (5 mL) in a separating funnel for extraction. Extract liquid was gently washed with distilled water repeatedly to remove the dissolved NaOH to terminate the saponification process. The obtained ethyl acetate phase was the ASTA-rich solution. AB-8 resin with weak polarity was used for ASTA purification. Macroporous resin was soaked in anhydrous ethanol for 24 h and washed with ultrapure water to remove ethanol. The treated AB-8 resin and ethyl acetate extract liquid were filled in a glass column by wet method. Water-soluble impurities, such as polysaccharide, were removed with ultrapure water of 2 BV, followed by the elimination of water with anhydrous ethanol of 1 BV. The desorption of resin and crude product was achieved by the addition of ethyl acetate. Then the mixture sample was filled in a glass column by dry method. The column chromatography silica gel (200–300 mesh) was mixed with n-hexane and the extracting solution. After gradient elution with n-hexane and acetone (50:1 → 1:1), free ASTA was collected.

Preparation of ASTA-NLC

Material Screening and Preformulation Study

The suitability of different materials for the formulation of NLC was assessed based on different considerations. The types of lipid and emulsifier were shown in Table II. An excessive amount of ASTA was added to the tested material and shaken for 24 h. The sample was centrifuged at 10000 rpm for 3 min. An appropriate amount of supernatant was withdrawn and dissolved in methanol for the determination of ASTA content using HPLC. Solid lipids (1 g) were melted and added ASTA until ASTA could no longer be dissolved in 5 min. The amount of ASTA was noted. Formulations were evaluated based on PS, EE, and storage stability.

Preparation of ASTA-NLC

ASTA-NLC was prepared with solid lipid, liquid lipid, and emulsifiers using a hot homogenization and ultrasonication method (27). The solid lipid was melted at 80°C and added with liquid lipid and emulsifiers to form the oil phase. The mixture was stirred at 80°C and added with the ASTA gradually. Ultrapure water was slowly dropped into the mixed oil phase, and the mixture was homogenized using ultrasonication at 400 W for 3 min. The obtained sample was cured in cold water for 5 min and preserved at 4°C for further study. The formulations of ASTA-NLC were listed in Table III.

Characterization of NLC

Particle Size and Polydispersity Index Analysis

A laser particle size analyzer (Zetasizer Nano ZS, Malvern Panalytical, Malvern, England) was used to determine the physical attributes of ASTA-NLC including PS, polydispersity index (PDI), and zeta potential. After diluting ASTA-NLC (2.5 mg/mL, 1 mL) with pure water into 5 mL, the sample was analyzed at 25°C and a scattering angle of 90°. The measurements were carried out in triplicate.

Encapsulation Efficiency

The EE% of ASTA-NLC was determined using a microcolumn centrifugation method (28). ASTA-NLC (0.2 mL) was diluted to 5 mL with methanol to serve as pre-column solution. Two pieces of wetted filter paper were placed at the bottom of a 2-mL syringe without cap. Swelled Sephadex G-50 was enclosed in the syringe, and the height of column was 4.9 cm. The column was balanced with ultrapure water for 5 min and then centrifuged at 2000 rpm for 3 min. ASTA-NLC (0.2 mL) was loaded into the column by centrifuging at 1000 rpm for 1 min. Ultrapure water (0.5 mL) was added to the column slowly and centrifuged at 1000 rpm for 3 min. The elution operation was repeated for 5 times. The obtained solution was diluted to 5 mL by methanol. The ASTA content was analyzed by HPLC. The EE of the drug was calculated though the Eq. (1).

$$EE(\%) = \frac{C_2}{C_1} \times 100\% \quad (1)$$

where C_1 was the content of ASTA in pre-column solution and C_2 was the content of ASTA in post-column solution. The measurements were run in triplicate.

Short-Term Storage Stability

The prepared ASTA-NLC was placed at room temperature for several days to observe whether there was precipitation or flocculation in the system.

Table II. Formulation parameters for the preparation of ASTA-NLC

Formulation parameter	Condition
Type of solid lipid	Stearic acid, glyceryl monostearate, and GTB
Type of liquid lipid	Soybean oil, isopropyl myristate, oleic acid, and Myl 812
Type of emulsifier	EL 35, F68, and Tween-80
Total lipid content (%, w/w)	3, 5, 7, and 10
Solid:liquid lipid ratio (w/w)	95:5, 80:20, 70:30, 60:40 ,and 50:50
Total lipid:drug ratio (w/w)	97:3, 95:5, 93:7, 90:10, and 85:15
Composite emulsifier ratio	EL 35:F68 = 2:1, 1:1 and 1:2; EL 35:Tween-80 = 1:1

ASTA-NLC, astaxanthin nanostructured lipid carrier; GTB, glyceryl tribehenate; Myl 812, decanoyl/octanoyl-glycerides; EL 35, Cremophor EL 35; F68, Pluronic F68

Transmission Electron Microscopy

Transmission electron microscopy (TEM, JEM-2100, FEI, Electronics Corporation, Japan) was employed to analyze the morphology of ASTA-NLC. A drib of diluted ASTA-NLC (2.5 mg/mL) with ultrapure water was dropped on a copper grid and stained with 2% phosphotungstic acid for 3 min. Excess liquid was removed from the sample with filter paper and dried at 25°C. The staining process was conducted twice. The morphology and PS of ASTA-NLC were observed under TEM.

Drug Release In Vitro

ASTA-NLC (10 mL) and ASTA ethanol solution (10 mL) equivalent to 21 mg ASTA were added to an activated dialysis bag (molecular retention 8000–14,000 Da, Union Carbide Corporation, USA), respectively. Dialysis bags were placed in phosphate buffer solution (PBS) solution with 0.3% sodium dodecyl sulfate (100 mL, pH 7.4) and stirred (100 rpm, 37 ± 1°C). Recipient medium (1 mL) was sampled at predetermined time intervals (0.5, 1, 2, 3, 4, 6, 8, 10, 12, 24, and 48 h), and a same volume of fresh medium was

Table III. Influence of changing formulation parameters on dosage form ($n = 3$, mean ± SD)

S. No.	Solid:liquid lipid ratio[a]	Total lipid: drug ratio	Total lipid content (%, w/w)	Type of emulsifier	Emulsifier concentration (%, w/w)	Composite emulsifier ratio	PS (nm)	EE (%)	Stability[b]
1	95:5	95:5	7	EL 35	3	/	65.1 ± 2.44	59.2 ± 5.10	+ + +
2	80:20	95:5	7	EL 35	3	/	72.7 ± 1.32	78.3 ± 3.35	- - -
3	70:30	95:5	7	EL 35	3	/	80.4 ± 2.43	85.8 ± 3.90	- - -
4	60:40	95:5	7	EL 35	3	/	90.9 ± 4.33	79.5 ± 3.42	- - -
5	50:50	95:5	7	EL 35	3	/	121.7 ± 2.03	76.6 ± 3.58	- - -
6	70:30	97:3	7	EL 35	3	/	73.2 ± 2.32	90.5 ± 5.73	- - -
7	70:30	95:5	7	EL 35	3	/	78.8 ± 2.74	84.7 ± 3.42	- - -
8	70:30	93:7	7	EL 35	3	/	83.6 ± 2.14	82.2 ± 2.83	- - -
9	70:30	90:10	7	EL 35	3	/	77.7 ± 2.00	62.9 ± 2.51	- - -
10	70:30	85:15	7	EL 35	3	/	69.3 ± 3.48	48.9 ± 3.55	+ + +
11	50:50	95:5	3	EL 35	3	/	49.2 ± 2.86	41.5 ± 4.75	- - -
12	50:50	95:5	5	EL 35	3	/	72.7 ± 2.37	58.0 ± 3.96	- - -
13	50:50	95:5	7	EL 35	3	/	119.5 ± 1.81	77.3 ± 3.69	- - -
14	50:50	95:5	10	EL 35	3	/	367.5 ± 5.11	63.4 ± 4.42	+ + +
16	70:30	97:3	7	EL 35	3	/	75.6 ± 2.97	89.6 ± 5.31	- - -
17	70:30	97:3	7	F68	3	/	643.2 ± 5.01	47.7 ± 3.20	+ + +
18	70:30	97:3	7	Tween-80	3	/	468.5 ± 7.18	53.4 ± 3.36	+ + +
19	70:30	97:3	7	EL 35:Tween-80	3	1:1	95.3 ± 2.67	86.1 ± 4.84	- - -
20	70:30	97:3	7	EL 35:F68	3	2:1	68.7 ± 2.72	93.6 ± 4.12	- - -
21	70:30	97:3	7	EL 35:F68	3	1:1	99.4 ± 3.01	93.7 ± 3.61	- - -
22	70:30	97:3	7	EL 35:F68	3	1:2	132.2 ± 3.92	91.4 ± 3.95	- - -

EL 35, Cremophor EL 35; F68, Pluronic F68; PS, particle size; EE, encapsulation efficiency
[a] *Glyceryl tribehenate (GTB):Decanoyl/octanoyl-glycerides (Myl 812)*
[b] *No crystal observed within 7 days; + crystal observed within 7 days*
—: no crystal observed within 21 days; +++: crystal observed within 21 days

added. All samples were filtered through 0.22-μm nylon membrane filters and analyzed by HPLC. The cumulative release percentages of ASTA were calculated and plotted against time.

Equilibrium Solubility

ASTA-NLC was freeze-dried to remove moisture. Excess ASTA and ASTA-NLC were respectively added to water (1 g) and oscillated in a thermostatic oscillator for 24 h (100 rpm, 25°C). Then they were centrifuged at 10000 rpm for 10 min. The supernatant was taken. ASTA-NLC was demulsified and diluted to measure the content of drug. ASTA was measured the content of drug directly.

Storage Stability

The storage stability of ASTA-NLC was assessed by variations in sample mass, PS, and EE with time. ASTA-NLC (5 mL) was divided into three groups, oxygen group, temperature group, and light group with three samples in each group. Oxygen group samples were stored in a ventilated chamber with a consistent temperature (25°C) and kept away from light. Temperature group samples were stored in a sealed bag under a constant temperature (37°C) and kept away from light. Light group samples were sealed at 25°C and exposed to ultraviolet light. The residual content of ASTA for each sample was measured at predetermined time intervals. The PS and EE of ASTA-NLC were recorded. The loss rates of ASTA were calculated using the Eq. (2).

$$loss(\%) = \frac{ASTA_{total} - ASTA_{residual}}{ASTA_{total}} \times 100\% \quad (2)$$

In Vitro Activity of ASTA-NLC

Demulsification of ASTA-NLC

Demulsification was applied to ASTA-NLC to provide a complete release of ASTA before the determination of antioxidant activity. ASTA-NLC (5 mL) was added with a same amount of methanol and demulsified by 400 W ultrasonication for 5 min. The liquid sample obtained from demulsification was used for antioxidant tests.

Total Antioxidant Capacity

2,2′-Azino-bis(3-ethylbenzothiazoline-6-sulfonic acid) (ABTS)-free radical scavenging method (29) was used to test the antioxidant property of the liquid sample obtained from demulsification. ABTS-free radical reserve solution was obtained by mixing ABTS (7.4 mmol/L) and $K_2S_2O_8$ (2.6 mmol/L) (1:1, v/v). The mixed solution was placed in dark at room temperature for 16 h. After diluting with ethanol, the liquid sample obtained from demulsifications (2 mL) of different concentrations was mixed with ABTS (2 mL), respectively, and kept from light for 10 min. The absorbance of each sample was measured at 734 nm by ultraviolet-visible spectrophotometer (UV2800PC, Shanghai Shunyu Hengping Scientific Instrument Limited Company, China). Pure ethanol was used as the blank control. Standard ASTA and VE were used as the positive controls.

The Total Reducing Power

$K_3[Fe(CN)_6]$ was used to determine the reducing capacity of ASTA-NLC according to the reference (30). The liquid sample obtained from demulsifications (2 mL) of different concentrations was added with ethanol in test tubes. Each sample was mixed with PBS (2.5 mL, 0.2 mol/L, pH 6.6) and $K_3[Fe(CN)_6]$ solution (2.5 mL, 1.0%), followed by the maintenance in a 50°C water bath for 20 min. The mixed solution was added with trichloroacetic acid (TCA, 2.5 mL, 10%) and centrifuged at 3000 rpm for 10 min. Supernatant (2 mL) was withdrawn and added with ethanol (2 mL) and $FeCl_3$ (1 mL, 0.1%). The sample was allowed to rest for 10 min after mixing, and the UV absorbance was measured at 700 nm. Pure ethanol was used as the blank control. Standard ASTA and VE were used as the positive controls.

Anti-linoleic Acid Lipid Peroxidation

The anti-linoleic acid lipid peroxidation property of ASTA-NLC was assessed by the established method (31). Linoleic acid (1.5 mL), tween-80 (1.5 mL), and PBS (100 mL, 0.05 mol/L, pH 7.0) were mixed uniformly. Such solution (1 mL) was taken out and added with PBS (2 mL) and the liquid sample obtained from demulsifications (1 mL) with different concentrations. Then the mixture was placed at room temperature for 20 min. Following, it was added with $FeSO_4$ solution (1 mL, 1 mmol/L) and kept at 37°C for 3 h. Obtained sample (1 mL) was mixed with TCA solution (1 mL, 10%). After incubation for 10 min, the system was added with 2,4,6-tribromoanisole (TBA) solution (2 mL, 0.67%) and placed in boiling water bath for 15 min. Finally, the sample was centrifuged at 3000 rpm for 10 min. The supernatant was taken and the UV absorbance was measured at 532 nm. DMSO was used as blank control. Standard ASTA and VE were used as positive controls.

In Vitro Skin Permeation and Retention Studies

Preparation of In Vitro Skin

The preparation of *in vitro* skin was in accordance with previous method (32). The dorsal hair of SD rats was removed. The rats were humanely killed after 24 h, and the dorsal skin was excised. Connective and adipose tissue under the skin were removed. The skin was washed with normal saline before permeation experiments.

Determination of Skin Penetration

Franz diffusion cell (Shenyang Yuwang Chemical Glass Instrument Limited Company, China) with an effective diffusion area of 2.3 cm^2 was used to perform the *in vitro* skin permeation study (32 ± 1°C). The skin sample was clamped between the donor and receptor chamber of the diffusion cell with the stratum corneum facing the donor chamber. ASTA-NLC (1 mL) was applied on the donor

compartment. Receptor chamber was filled with PBS (7 mL, pH 7.4) containing 50% ethanol. The receptor medium was stirred at 400 rpm throughout the experiment. For each experiment, receptor solution (1 mL) was sampled at predetermined time intervals (0.5, l, 2, 4, 6, 8, 10, 12, and 24 h), and then the same volume of PBS was immediately added into the receptor chamber. The ASTA concentration of all samples was analyzed by HPLC. Control experiment was conducted with 50% ethanol solution containing the same amount of ASTA. The penetration of the drug (Q) was calculated by the Eq. (3).

$$Q(\%) = \frac{C_m V + \sum_{i=1}^{n-1} C_i V_i}{A} \times 100\% \quad (3)$$

where A was the effective penetration area, V was the volume of the receiving medium, V_i was the volume of withdrawn sample, C_i was the cumulative drug concentration in the receiving medium at the first and last sampling, and C_m was the drug concentration in the receiving medium at the time of the sampling.

Determination of Skin Retention

After the *in vitro* transdermal test, the effective transdermal part of skin was washed and cut into pieces. The samples were added with normal saline (15 mL) and treated under ultrasonication for 30 min (50°C, 300 W). The solution was then filtered through a 0.45-μm nylon membrane and diluted to 100 mL, and the ASTA concentration was analyzed by HPLC. The drug retention rate was calculated according to the Eq. (4).

$$retention(\%) = \frac{Q_2}{Q_1} \times 100\% \quad (4)$$

where Q_1 was the total input amount of ASTA and Q_2 was the retaining amount of ASTA in the skin.

Skin Irritation Test

According to the method described in the literature (33), KM mice ($n = 6$) were subjected to dermal irritancy testing and were individually caged. The left ear of each mouse was applied with 0.1% ASTA-NLC (10 mg), while the right ear was left untreated as a control group. After 24 h, the erythema and ear edema tests were conducted using a magnifying glass and a digital caliper (Meinaite, China), respectively. The tests were performed for 7 days during which the scoring was performed daily. According to Uttley (34), the erythema was graded: 0, no visible blood vessels or erythema; 2, few blood vessels, no erythema; 4, main vessels visible and slight erythema; and 10, pronounced blood vessels and marked erythema.

Statistical Analysis

All results were expressed as mean ± SD and analyzed using origin 9.1 and SPSS. Multiple comparisons were conducted using one-way or two-way ANOVA analysis. A student's t test was performed to determine the statistical significance between experimental groups. A value of $p < 0.05$ was considered to be statistically significant.

RESULTS

Solubility of ASTA in Different Lipid Materials

The solubility values of ASTA in different solid lipids were GTB (28.76 mg/g) > glyceryl monostearate (25.49 mg/g) > stearic acid (7.91 mg/g). ASTA solubilities in the liquid lipids were isopropyl myristate (49.41 mg/g) > Myl 812 (40.90 mg/g) > soybean oil (11.31 mg/g) > oleic acid (2.68 mg/g). ASTA solubilities in different emulsifiers were EL 35 (1.62 mg/g) > F68 and Tween-80, which were lower than that in lipid materials. The solubility values of ASTA in in F68 and Tween-80 were beyond the detection range of the standard curve. These results suggested the suitability to load ASTA into lipid materials while with minimal distribution into the emulsifier phase.

Material Selection

The selection of composition materials was based on the PS of NLC formulated. The PS of ASTA-NLC formulated with stearic acid as solid lipid was 478.2 nm, and the size was not favorable for transmembrane delivery. Phase separation and flocculation occurred during the cooling and curing process. The PS of ASTA-NLC formulated with glyceryl monostearate as solid lipid was 59.7 nm, but the system broke into different layers within 1 day. The ASTA-NLC formulated with GTB as solid lipid had small PS (69.3 nm), and the system was stable after 7 days. Therefore, GTB was selected as the solid lipid for further study. The PS of ASTA-NLC formulated with liquid lipid was Myl 812 (65.8 nm) < isopropyl myristate (74.0 nm) < soybean oil (79.4 nm) < oleic acid (93.6 nm). Myl 812 and GTB have certain similarities in chemical structure, which enables them to be miscible well (24). Finally, combining with the solubility of astaxanthin in different excipients, GTB and Myl 812 were selected as the lipid materials for preparation of ASTA-NLC.

Optimization of Formulation

According to the PS, EE, and stability of ASTA-NLC, total lipid concentration, solid:liquid lipid ratio, total lipid:drug ratio, type of emulsifier, and composite emulsifiers ratio were assessed to determine the optimal formulation (Table III). N21 was selected as the optimal formulation (Table IV).

Characterization of ASTA-NLC

Particle Size and Morphology of ASTA-NLC

The TEM morphology of ASTA-NLC revealed a homogeneous size, spherical shape, and small single-chamber structure (Fig. 2a). The average PS of ASTA-NLC was determined to be 67.4 ± 2.1 nm ($n = 3$) with an acceptable PDI of 0.26. The PS distribution was narrow (Fig. 2b). ASTA-

Table IV. Prescription process of ASTA-NLC

Material	Content
ASTA	210 mg
Glyceryl tribehenate	4.9 g
Decanoyl/octanoyl-glycerides	2.1 g
Cremophor EL 35	2 g
Pluronic F68	1 g
Distilled water	100 mL

ASTA, astaxanthin; NLC, nanostructured lipid carrier; GTB, glyceryl tribehenate; Myl 812, decanoyl/octanoyl-glycerides; EL 35, Cremophor EL 35; F68, Pluronic F68

NLC was clear and transparent with orange opalescence (Fig. 2c).

Encapsulation Efficiency of ASTA-NLC

The EE% of ASTA-NLC was determined to be 94.3 ± 0.5%.

In Vitro Drug Release of ASTA-NLC

The effect of NLC on the release of ASTA was investigated *in vitro* by determining the drug release across a dialysis bag. In general, the drug release rate of ASTA-NLC was significantly lower than that of ASTA solution (Fig. 3), showing a sustained release profile effectively up to 48 h. In detail, 4.5 ± 2.0% of ASTS was released from the formulation within 0.5 h, compared with the 19.4 ± 3.2% for crude ASTA. The complete dissolution of ASTA was achieved within 4 h, while at the same time, ASTA-NLC showed a cumulative release of approximate 28.7 ± 1.7%. The drug release of ASTA-NLC showed a steady increase until reaching a plateau at 24 h. The final drug release percent was maintained at about 83.0 ± 3.4%.

Equilibrium Solubility

Drug in ASTA was not detected by HPLC. Equilibrium solubility of the drug in ASTA-NLC was 4.7 mg/g.

Storage Stability of ASTA-NLC

The incorporation of ASTA in NLC protected ASTA from exposure to oxygen, heating, and ultraviolet light effectively (Fig. 4). As seen Fig. 4a, the content loss of ASTA in a solution form showed a linear increase within 12 h and reached 85.3 ± 3.1% as compared with the 12.0 ± 2.0% of ASTA-NLC. At 24 h, essentially all unformulated ASTA was oxidized, while the drug content loss of ASTA-NLC was only 15.5 ± 2.6%. The partial degradation of ASTA reduced the EE of ASTA-NLC by 1.8% and increased the PS by 6.6%. The effect of heating on the loss rates of ASTA was shown in Fig. 4b. Both unformulated ASTA and ASTA-NLC showed gradual degradation within the investigated time range. After 6 days, the degradation rate of crude ASTA was approximately 79.4 ± 4.0%, compared with the 54.9 ± 3.8% of ASTA-NLC. Neither ASTA-NLC nor ASTA settled or accumulated. The effect of ultraviolet irradiation on ASTA's loss rate in was shown in Fig. 4c. After an exposure for 9 h, the loss rate of drug in ASTA-NLC was 83.1 ± 3.6%, while the ASTA in solution completely degraded. At the end of experiment, the PS of ASTA-NLC increased by 22.7%, and the EE decreased by 74.5%.

In Vitro Activity of ASTA-NLC

As could be seen from Fig. 5, all types of activity of ASTA-NLC were consistent with standard ASTA at the same drug concentration. No decrease in *in vitro* activity was observed for ASTA due to the incorporation into NLC.

Total Antioxidant Capacity

The ABTS• scavenging ability of ASTA was slightly higher than that of VE in the concentration range of 20 to 60 mg/L and positively correlated with the concentration of the sample (Fig. 5a). Outside of this range, VE was more active than ASTA and ASTA-NLC.

The Total Reducing Capacity

The total reduction capacity of ASTA-NLC and ASTA was both much higher than that of VE in the same concentration range of 5 ~ 25mg/L and increased significantly with concentration (Fig. 5b). The changing profiles of ASTA and ASTA-NLC were highly comparable with each other.

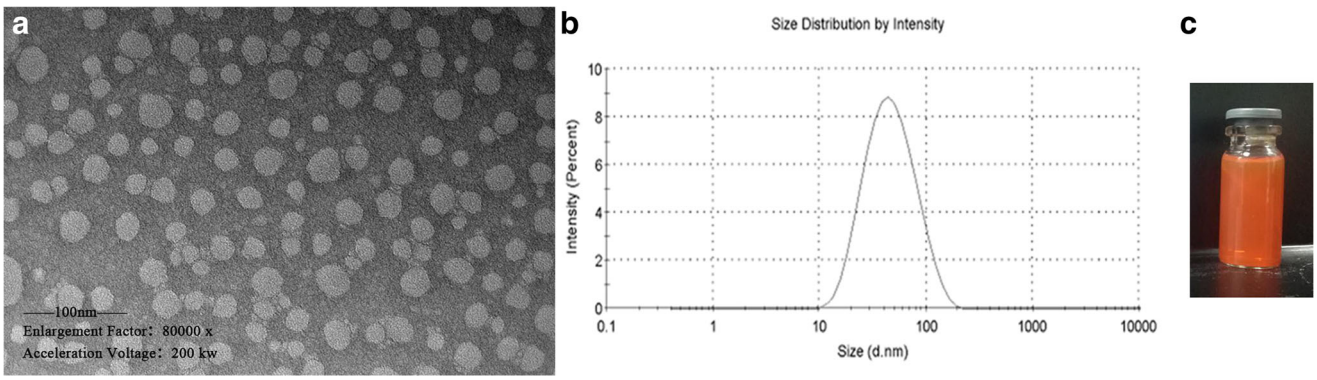

Fig. 2. **a** TEM image of ASTA-NLC, **b** particle size distribution of ASTA-NLC, and **c** the appearance evaluation of ASTA-NLC

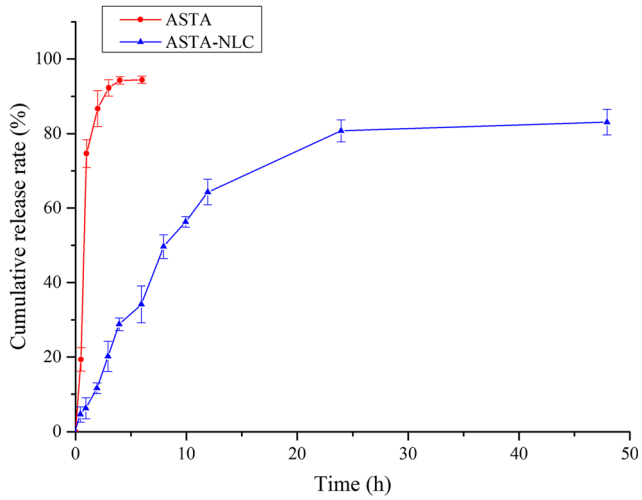

Fig. 3. *In vitro* drug release profiles of ASTA and ASTA-NLC

Anti-linoleic Acid Lipid Peroxidation

The inhibitory activity of ASTA-NLC and ASTA on MDA in the range of 100~600 mg/L was both stronger than that of VE in the same concentration (Fig. 5c). The changing profiles of ASTA and ASTA-NLC were highly comparable with each other.

In Vitro Skin Retention and Permeation Studies

Determination of Skin Penetration

The dynamic fitting equation was obtained by taking the permeability (Q) per unit area as the ordinate and the penetrative time (t) as the abscissa and performing a linear regression. The result was shown as the curve of cumulative permeability (Fig. 6). ASTA-NLC was able to permeate through skin at a constant rate within 0~12 h. Cumulative permeability at 24 h was 174.10 ± 4.38 μg/cm^2 (18.70% of drug input). Compared with ASTA-NLC, unformulated ASTA was able to permeate at a larger rate within 0~12 h. Cumulative permeability at 24 h was 295.20 ± 6.04 μg/cm^2 (31.71% of drug input).The results showed that the transdermal absorption of ASTA-NLC was significantly different from that of the control preparation, and the cumulative transdermal amount within 24 h was lower than that of ASTA solution.

Determination of Skin Retention

After calculation, the drug retention in rat skin was 18.64 ± 1.64 μg/cm^2 within 24 h for ASTA-NLC. And the retention of ASTA in rat skin was 8.00 ± 1.62 μg/cm^2 within 24 h. The skin retention of ASTA-NLC was effectively increased by 2.33-fold.

Skin Irritation Test

No allergic ear erythema or edema was observed within the investigated timescale. No systemic allergic reactions such as asthma, standing instability, or shock occurred. The sensitization rate of ASTA-NLC was zero.

DISCUSSION

Preparation of ASTA-NLC

Major materials for NLC formulations include solid lipids, liquid lipids, and emulsifiers. Solid lipids have been selected based on the biodegradability, physiological compatibility, morphological support in terms of forming spherical pellets, and storage stability. Liquid lipids play an important role in improving drug loading, encapsulation efficiency (EE), and physical stability of the payload. On that note, fatty acid esters of medium or long chains were selected accordingly. Multiple emulsifying agents have been selected to prepare composite emulsifier to improve EE, particle size (PS) distribution, and storage stability of nanoparticles. The solubility values of ASTA in different lipid and emulsifier materials were firstly measured in order to ensure that ASTA can be dissolved in these carriers during the formulation process.

Optimization of ASTA-NLC

Particle Size and Morphology of ASTA-NLC

The small size of ASTA-NLC (67.4 ± 2.1 nm) and homogeneous size distribution have been considered a result of the physiochemical properties of lipid materials and good drug-lipid miscibility as indicated by the ASTA solubility values. The miscibility between the selected solid and liquid lipid (GTB and Myl 812) could be due to the similarity in their chemical structures (15). In addition to the effect of

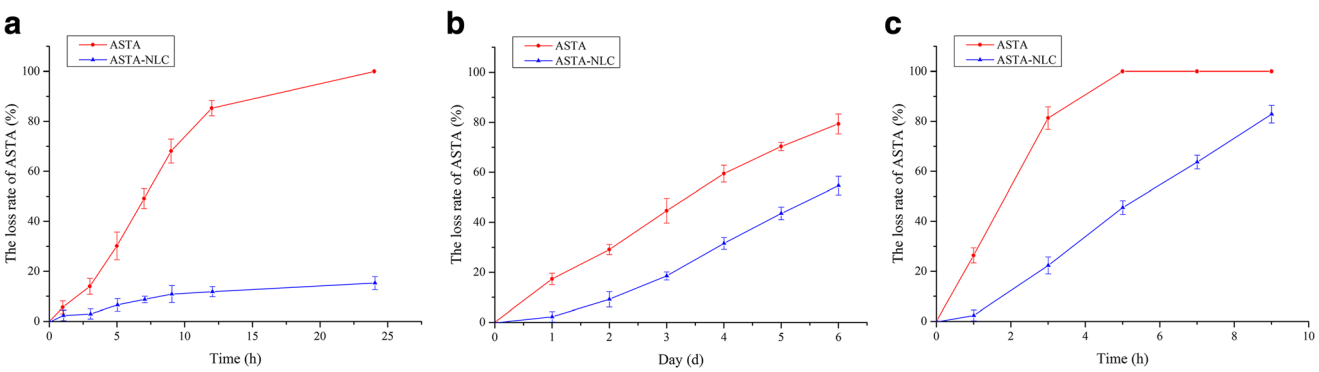

Fig. 4. Effect of **a** oxygen, **b** heating, and **c** ultraviolet light on drug content loss in ASTA solution and ASTA-NLC

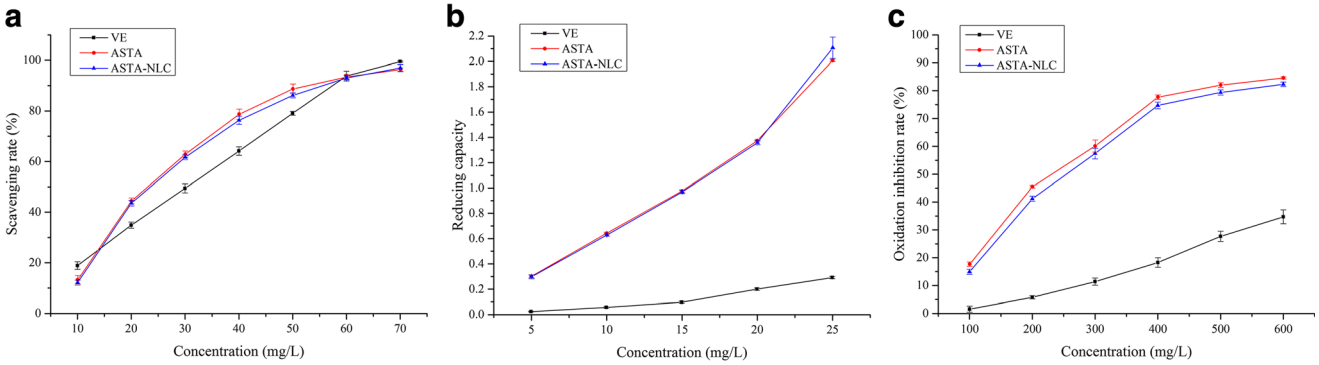

Fig. 5. Antioxidative activity of ASTA, ASTA-NLC, and VE revealed by **a** scavenging ability of ABTS•, **b** total reducing capacity, and **c** inhibitory effect on MDA

ASTA solubility in lipid carrier, the incorporation of ASTA may change the size dimensions of ASTA-NLC by altering the geometric packing (35) through its distribution in the physical gap between chains of triglyceride fatty acid and solid lipid. On that note, the ideal miscibility between drug, solid lipid, and liquid lipid eliminates the occurrence of phase separation among different compositions and thereby improves the size distribution of ASTA-NLC. The composite emulsifier was composed of EL 35 and F68, both of which provide a limited solubility for ASTA, maximizing the drug distribution in the inner lipid matrix. EL 35 and F68 have also been well recognized to increase the dispersibility of ASTA-NLC in aqueous media due to their amphiphilic characteristics (36). The ideal size and monodisperse profile of ASTA-NLC are expected to benefit the transdermal absorption, as it is more effective (37) for smaller particles to penetrate the skin barrier and reach the dermis.

In Vitro Drug Release of ASTA-NLC

The release of ASTA from ASTA-NLC is sustained compared with material drug. The slower release rate is a result of NLC incorporation. Drug release from insoluble carriers follows a diffusion-controlled mechanism upon erosion of lipid matrix (38). The melted blend (39) of solid lipid and liquid lipid increased the viscosity of the particle matrix, leading to a slower drug release rate. The sustained drug release profile of ASTA-NLC is expected to provide a prolonged therapeutic effect and protection of ASTA from oxygen, heating, and ultraviolet exposure when applied to skin (40).

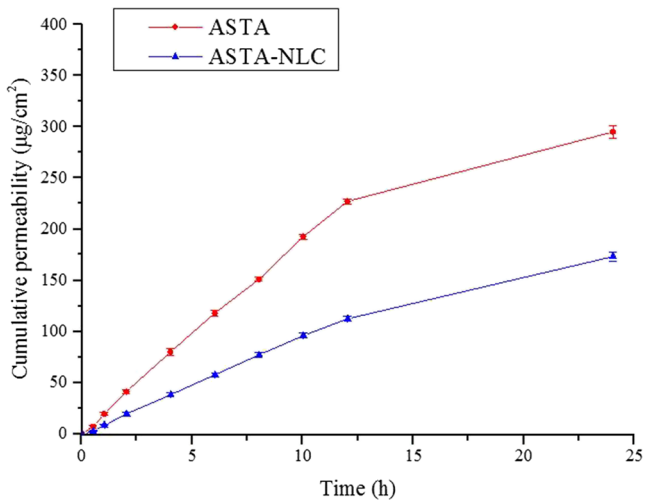

Fig. 6. *In vitro* cumulative skin permeation of ASTA and ASTA-NLC

Encapsulation Efficiency of ASTA-NLC

EE is one of the most vital indicators for evaluating the quality of NLC and associated preparation method. The EE of ASTA-NLC in this study (94.3 ± 0.5%) suggested effective drug encapsulation behavior. Similar to the attribute to size distribution, the high solubility of ASTA in lipid carriers and low solubility in emulsifier should be a reason for the effective encapsulation. Such solubility difference ensured that ASTA could readily distribute into lipid phases to complete drug encapsulation, with minimizing partition into emulsifiers. Increasing the total oil content could improve the drug loading of NLC, but in order to ensure drug stability and small PS, the content of emulsifier is increased accordingly. With the increase in the amount of liquid lipids, the disordered spatial structure (41) become loose, which is favorable for drug incorporation and storage. Overall, the EE results were corresponding to the size distribution of ASTA-NLC, justifying the practicability of designed formulation and preparation methods.

Equilibrium Solubility

ASTA is a lipid-soluble carotenoid, which was insoluble in water. So its content in water after equilibrium could not detected by HPLC. ASTA-NLC is a new formulation in which the water is a continuous phase. The lipids that contain the drug dispersed evenly in the water, thus allowing more of the drug to be dissolved.

Storage Stability of ASTA-NLC

ASTA-NLC can effectively protect the drug payload from oxygen during storage. Such stability profile of ASTA-NLC suggested the feasibility to apply the formulations on skin under ambient condition for a prolonged time, during which ASTA could be constantly absorbed. Under the exposure to high temperature, the particle motion is

accelerated, and ASTA-NLC is observed to aggregate to increase PS and decrease EE. Nevertheless, the thermal stability of ASTA is still effectively improved through the encapsulation into NLC. Under ultraviolet irradiation, the stability of ASTA is enhanced by the physical barrier provided by the NLC structure. The maintenance of ASTA content in a formulation is a prerequisite for the proposed biological activity, and thus, the therapeutic effect of ASTA is expected to benefit from the NLC formulation. Based on all results, it is suggested that ASTA-NLC is stored hermetically in low temperature and dark condition, in the best effort to improve ASTA stability.

In Vitro Activity of ASTA-NLC

In general, the *in vitro* activities of ASTA, including antioxidant, reduction, and anti-linoleate lipid peroxidation, are effectively preserved after encapsulation into NLC. The ability of ASTA-NLC to remove ABTS-free radicals and total reduction capacity (42) of the hydrogen atom transfer reaction are essentially the same as material drug. These two antioxidant indicators are often used to compare the antioxidant capacity of food and medicinal plant extracts and to test the property change induced by dosage forms. Similarly, for the inhibitory effect on MDA, no obvious change in ASTA ability is induced by the NLC encapsulation. The experimental results showed that the *in vitro* activity of ASTA was not compromised by the extraction of ASTA or preparation of ASTA-NLC. Since certain cosmetic benefits of ASTA, such as anti-inflammatory and antiapoptotic effects, are associated with the antioxidant ability of ASTA, the maintenance of ASTA activity is expected to preserve the therapeutic effects.

In Vitro Skin Permeation and Retention Studies

Before the skin penetration test, the compatibility of the recipient solution was verified to ensure that integrity of skin sample could be preserved during experiment. Previous literature (43) had shown that human skin remained its completeness upon contacting a receptor liquid containing 50% ethanol for 24 h. The apparent permeation of ASTA showed a disadvantageous reduction by the encapsulation in NLC, for which drug release could be a reason. The ASTA release from ASTA-NLC showed a sustained profile compared with unformulated ASTA, reducing the free drug that can readily permeate through the skin. However, the skin retention of ASTA is effectively improved by ASTA-NLC, maximizing the local ASTA concentration in skin while decreasing the systemic delivery (44). A plausible explanation for the high skin retention provided by ASTA-NLC is that NLC has high affinity to the cell membrane of skin due to its lipid components. The drug retention in skin can provide a prolonged drug release following a reservoir effect. According to the prior findings (45), ASTA is readily absorbed by dermal fibroblasts. In this regard, the improved skin retention of ASTA could be beneficial to skin targeting.

Skin Irritation Test

No sensitization was observed for ASTA-NLC within the investigated timescale. The result suggested an ideal biocompatibility of ASTA-NLC and the suitability of its topical application as a cosmeceutical.

CONCLUSION

In this study, a novel ASTA-NLC was successfully prepared with small particle size, uniform size distribution, high encapsulation efficiency, improved skin retention, and good stability against oxygen, heating, and ultraviolet exposure. The intrinsic antioxidant activity of ASTA was effectively preserved after the incorporation into designed NLC formulations. ASTA-NLC was able to concentrate in skin without skin damage, laying a fundamental foundation for its potential application as a cosmeceutical product. The cosmetic benefits of ASTA are expected to effectively perform through skin, owing to the improved transdermal delivery offered by ASTA-NLC.

ACKNOWLEDGMENTS

I would like to express my deep thanks and sincere gratitude to Jing Han, professor of Biochemistry, Faculty of Pharmaceutical Engineering, Shenyang Pharmaceutical University, for her support and effort in revising the paper.

COMPLIANCE WITH ETHICAL STANDARDS

Conflict of Interest The authors declare that they have no conflict of interest.

REFERENCES

1. Musa Y, Alime G, Cihangir U, Özlem YT, Levent T, Ahmi Ö, *et al*. Effects of astaxanthin on antioxidant parameters in arpe-19 cells on oxidative stress model. Int J Ophthalmol. 2019;12(6):930–6. https://doi.org/10.18240/ijo.2019.06.08.
2. Fakhri S, Abbaszadeh F, Dargahi L, Jorjani M. Astaxanthin: a mechanistic review on its biological activities and health benefits. Pharmacol Res. 2018;136:1–20. https://doi.org/10.18240/ijo.2019.06.08.
3. Zhang L, Wang H. Multiple mechanisms of anti-cancer effects exerted by astaxanthin. Mar Drugs. 2015;13(7):4310–30. https://doi.org/10.3390/md13074310.
4. Saravanan B, Elumalai A, Periyasamy V, Carani VA. Astaxanthin restricts weight gain, promotes insulin sensitivity and curtails fatty liver disease in mice fed a obesity-promoting diet. Process Biochem. 2010;45(8):1406–14. https://doi.org/10.1016/j.procbio.2010.05.016.
5. Ambati RR, Phang SM, Ravi S, Aswathanarayana RG. Astaxanthin: sources, extraction, stability, biological activities and its commercial applications. Mar Drugs. 2014;12(1):128–52. https://doi.org/10.3390/md12010128.
6. Dominique T, Jacqueline C, de Henauw S, Karen IH, John K, Alexandre M, *et al*. Safety of astaxanthin for its use as a novel food in food supplements. EFSA J. 2020;18(2):1–9. https://doi.org/10.2903/j.efsa.2020.5993.
7. Qingxin Z, Lu Y, Jie X. Studies on the digestion and absorption characteristics of esterified astaxanthins from *Haematococcus pluvialis*. J Chin Inst Food Sci and Technol. 2019;19(4):125–32. https://doi.org/10.16429/j.1009-7848.2019.04.015.

8. Yoko Y, Mati Ur R, Tadamichi S. Astaxanthin, a xanthophyll carotenoid, inhibits ultraviolet-induced apoptosis in keratinocytes. Exp Dermatol. 2014;23(3):178–83. https://doi.org/10.1111/exd.12347.
9. Suganuma K, Nakajima H, Ohtsuki M, Imokawa G. Astaxanthin attenuates the UVA-induced up-regulation of matrix-metalloproteinase-1 and skin fibroblast elastase in human dermal fibroblasts. J Dermatol Sci. 2010;58(2):136–42. https://doi.org/10.1016/j.jdermsci.2010.02.009.
10. Kumi T, Nobuko H, Mayuko F, Yu T, Yuki A. Protective effects of astaxanthin on skin deterioration. J Clin Biochem Nutr. 2017;61(1):33–9. https://doi.org/10.3164/jcbn.17-35.
11. Liu JL, Dai MQ, Yang Z, Li S, Zhang SC, Li J, *et al*. Effect of astaxanthin/natural DNA/chitosan nanoparticles on UV-induced photoaging of mouse skin. Chin J Mar Drugs. 2019;38(4):32–8. https://doi.org/10.13400/j.cnki.cjmd.2019.04.005.
12. Hong L, Zhou CL, Chen FP, Han D, Wang CY, Li JX, *et al*. Development of a carboxymethyl chitosan functionalized nanoemulsion formulation for increasing aqueous solubility, stability and skin permeability of astaxanthin using low-energy method. J Microencapsul. 2017;34(8):707–21. https://doi.org/10.1080/02652048.2017.1373154.
13. Susumu H, Kanako T, Yuko I, Shiota K, Ryota S, Asako Y, *et al*. Protective effects of topical application of a poorly soluble antioxidant astaxanthin liposomal formulation on ultraviolet-induced skin damage. J Pharm Sci. 2012;101(8):2909–16. https://doi.org/10.1002/jps.23216.
14. Ashwini G, Ryann C, Dunesh K, Amit T, Jeffrey NE, Harsh C. Preparation, Characterization, and In vitro evaluation of curcumin- and resveratrol-loaded solid lipid nanoparticles. AAPS PharmSciTech. 2019;20(4). https://doi.org/10.1208/s12249-019-1349-4.
15. Ghasemiyeh P, Azadi A, Daneshamouz S, Heidari R, Azarpira N, Mohammadi-Samani S. Cyproterone acetate-loaded nanostructured lipid carriers: effect of particle size on skin penetration and follicular targeting. Pharm Dev Technol. 2019;24(7):812–23. https://doi.org/10.1080/10837450.2019.1596133.
16. Chew BP, Mathison BD, Hayek MG, Massimino S, Reinhart GA, Park JS. Dietary astaxanthin enhances immune response in dogs. Vet Immunol Immunopathol. 2011;140(3–4):199–206. https://doi.org/10.1016/j.vetimm.2010.12.004.
17. Ellen KG, Rahul S, Mahantesh J, Sandeep J, Chunderika M, Suresh V, *et al*. Preparation and optimization of Meropenem-loaded solid lipid nanoparticles: in vitro evaluation and molecular modeling. AAPS PharmSciTech. 2017;18(6):2011–25. https://doi.org/10.1208/s12249-016-0675-z.
18. Aljaeid BM, Hosny KM. Fabrication and evaluation of phytomenadione as a nanostructure lipid carrier for enhancement of bioavailability. Pharm Dev Technol. 2018;23(4):382–6. https://doi.org/10.1080/10837450.2017.1312440.
19. Choi C-I. Astaxanthin as a peroxisome proliferator-activated receptor (PPAR) modulator: its therapeutic implications. Mar Drugs. 2019;17(4):242–53. https://doi.org/10.3390/md17040242.
20. Han Y, Li Y, Zhang P, Sun J, Li X, Sun X, *et al*. Nanostructured lipid carriers as novel drug delivery system for lung cancer gene therapy. Pharm Dev Technol. 2016;21(3):277–81. https://doi.org/10.3109/10837450.2014.996900.
21. Jenning V, Thünemann AF, Gohla SH. Characterisation of a novel solid lipid nanoparticle carrier system based on binary mixtures of liquid and solid lipids. Int J Pharm. 2000;199(2):167–77. https://doi.org/10.1016/s0378-5173(00)00378-1.
22. Chew BP, Park JS. Carotenoid action on the immune response1. J Nutr. 2004;134(1):257–61. https://doi.org/10.1093/jn/134.1.257s.
23. Li B, Ge ZQ. Nanostructured lipid carriers improve skin permeation and chemical stability of idebenone. AAPS PharmSciTech. 2012;13(1):276–83. https://doi.org/10.1208/s12249-011-9746-3.
24. Wang W, Chen L, Huang X, Shao A. Preparation and characterization of minoxidil loaded nanostructured lipid carriers. AAPS PharmSciTech. 2017;18(2):509–16. https://doi.org/10.1208/s12249-016-0519-x.
25. Iti C, Mohd Y, Madhu V, Alok PS. Nanostructured lipid carriers: a groundbreaking approach for transdermal drug delivery. Adv Pharm Bull. 2020;10(2):150–65. https://doi.org/10.34172/apb.2020.021.
26. Ji-ying Q, Yi-jing Y, Qin C, Jing H, Shi-bin Z. Optimization of ultrasonic extraction technology of astaxanthin from *Haematococcus pluvialis*. Food Ind Technol. 2015;36(6):313–6. https://doi.org/10.13386/j.issn1002-0306.2015.06.060.
27. Tran TH, Ramasamy T, Truong DH, Choi H-G, Yong CS, Kim JO. Preparation and characterization of fenofibrate-loaded nanostructured lipid carriers for oral bioavailability enhancement. AAPS PharmSciTech. 2014;15(6):1509–15. https://doi.org/10.1208/s12249-014-0175-y.
28. Feng F, Sun L, Wang J, Wang Y-Q, Wu Y, Zhang J-M, *et al*. Determination of main drug content and encapsulation rate in furandiene nanolipid carrier. Her Med. 2016;35:103–5. https://doi.org/10.3870/j.issn.1004-0781.2016.z1.047.
29. Campanini MZ, Custodio DL, Ivan AL, Martins SM, Paranzini MJ, Martinez RM, *et al*. Topical formulations containing Pimenta pseudocaryophyllus extract: in vitro antioxidant activity and in vivo efficacy against uv-b-induced oxidative stress. AAPS PharmSciTech. 2014;15(1):86–95. https://doi.org/10.1208/s12249-013-0049-8.
30. Xua L, Jia-Hui L, Yong-feng L. Antioxidant activity of chlorogenic acid extracted from peach blossom. Mod Chin Med. 2018;60(6):697–701. https://doi.org/10.13313/j.issn.1673-4890.20180131002.
31. Kangfei Y, Ruilian Z, Xiaojuan L, Yong C, Lichao Z, Liping H. Studies on anti-lipid peroxidation activity of different stereoisomeric astaxanthin. J Chin Inst Food Sci and Technol. 2018;18(10):86–94. https://doi.org/10.16429/j.1009-7848.2018.10.012.
32. Shetty PK, Manikkath J, Tupally K, Kokil G, Hegde AR, Raut SY, *et al*. Skin delivery of egcg and silibinin: potential of peptide dendrimers for enhanced skin permeation and deposition. AAPS PharmSciTech. 2017;18(6):2346–57. https://doi.org/10.1208/s12249-017-0718-0.
33. Ng SF, Anuwi NA, Tengku-Ahmad TN. Topical lyogel containing corticosteroid decreases ige expression and enhances the therapeutic efficacy against atopic eczema. AAPS PharmSciTech. 2015;16(3):656–63. https://doi.org/10.1208/s12249-014-0248-y.
34. Uttley M, Abbe NJV. Primaryirritation of skin – mouse ear test and human patch test procedures. J Soc Cosmet Chem. 1973;24(4):217–27 http://www.doc88.com/p-9292322370476.html.
35. Liu Y, Sun C, Li W, AduFrimpong M, Wang Q, Yu J, *et al*. Preparation and characterization of syringic acid-loaded tpgs liposome with enhanced oral bioavailability and in vivo antioxidant efficiency. AAPS PharmSciTech. 2019;20(98):98–107. https://doi.org/10.1208/s12249-019-1290-6.
36. Wei Q, Yang Q, Wang Q, Sun C, Zhu Y, Niu Y, *et al*. Formulation, characterization, and pharmacokinetic studies of 6-gingerol-loaded nanostructured lipid carriers. AAPS PharmSciTech. 2018;19(8):3661–9. https://doi.org/10.1208/s12249-018-1165-2.
37. Zhou X, Hao Y, Yuan L, Pradhan S, Shrestha K, Pradhan O, *et al*. Nano-formulations for transdermal drug delivery: a review. Chin Chem Lett. 2018;29(12):1713–24. https://doi.org/10.1016/j.cclet.2018.10.037.
38. Khan S, Baboota S, Ali J, Khan S, Narang RS, Narang JK. Nanostructured lipid carriers: an emerging platform for improving oral bioavailability of lipophilic drugs. Int J Pharm Investig. 2015;5(4):182–91. https://doi.org/10.4103/2230-973X.167661.
39. Chinsriwongkul A, Chareanputtakhun P, Ngawhirunpat T, Rojanarata T, Sila-on W, Ruktanonchai U, *et al*. Nanostructured lipid carriers (NLC) for parenteral delivery of an anticancer drug. AAPS PharmSciTech. 2012;13(1):150–8. https://doi.org/10.1208/s12249-011-9733-8.
40. Ling JTS, Roberts CJ, Billa N. Antifungal and mucoadhesive properties of an orally administered chitosan-coated amphotericin b nanostructured lipid carrier (nlc). AAPS PharmSciTech. 2019;20(3):136. https://doi.org/10.1208/s12249-019-1346-7.
41. Talegaonkar S, Bhattacharyya A. Potential of lipid nanoparticles (slns and nlcs) in enhancing oral bioavailability of drugs with poor intestinal permeability. AAPS PharmSciTech. 2019;20(3):121. https://doi.org/10.1208/s12249-009-9193-6.

42. Zampini IC, Ordonez RM, Isla MI. Autographic assay for the rapid detection of antioxidant capacity of liquid and semi-solid pharmaceutical formulations using abts*+ immobilized by gel entrapment. AAPS PharmSciTech. 2010;11(3):1159–63. https://doi.org/10.1208/s12249-010-9484-y.
43. D'Angelo Costa GM, Sales de Oliveira Pinto CA, Rodrigues Leite-Silva V, Rolim Baby A, Robles Velasco MV. Is vitamin D3 transdermal formulation feasible? An ex vivo skin retention and permeation. AAPS PharmSciTech. 2018;19(5):2418–25. https://doi.org/10.1208/s12249-018-1065-5.
44. Kelchen MN, Brogden NK. *In vitro* skin retention and drug permeation through intact and microneedle pretreated skin after application of propranolol loaded microemulsions. Pharm Res. 2018;35(12):228–40. https://doi.org/10.1007/s11095-018-2495-1.
45. Emanuela C, Arianna M, Claudia F, Felicitas D, Mauro P, Helmut S, *et al*. Astaxanthin, canthaxanthin and b-carotene differently affect uva-induced oxidative damage and expression of oxidative stress-responsive enzymes. Exp Dermatol. 2009;18(3):222–31. https://doi.org/10.1111/j.1600-0625.2008.00790.x.